HHS Public Access

Author manuscript

*J Bone Miner Res*. Author manuscript; available in PMC 2016 April 10.

Published in final edited form as:

*J Bone Miner Res*. 2016 April ; 31(4): 864–873. doi:10.1002/jbmr.2733.

# Deletion of Rac in Mature Osteoclasts Causes Osteopetrosis, an Age-Dependent Change in Osteoclast Number, and a Reduced Number of Osteoblasts In Vivo

**Meiling Zhu**[1], **Ben-hua Sun**[1], **Katarzyna Saar**[1], **Christine Simpson**[1], **Nancy Troiano**[2], **Sarah L Dallas**[3], **LeAnn M Tiede-Lewis**[3], **Erin Nevius**[4], **João P Pereira**[4], **Robert S Weinstein**[5], **Steven M Tommasini**[2], and **Karl L Insogna**[1]

[1]Department of Internal Medicine, Endocrinology, Yale School of Medicine, New Haven, CT, USA

[2]Department of Orthopaedics and Rehabilitation, Yale School of Medicine, New Haven, CT, USA

[3]Department of Oral and Craniofacial Sciences, School of Dentistry, University of Missouri, Kansas City, Kansas City, MO, USA

[4]Department of Immunobiology, Yale School of Medicine, New Haven, CT, USA

[5]Department of Internal Medicine, University of Arkansas for Medical Sciences and the Central Arkansas Veterans Health Care System, Little Rock, AR, USA

## Abstract

Rac1 and Rac2 are thought to have important roles in osteoclasts. Therefore, mice with deletion of both Rac1 and Rac2 in mature osteoclasts (DKO) were generated by crossing $Rac1^{flox/flox}$ mice with mice expressing Cre in the cathepsin K locus and then mating these animals with $Rac2^{-/-}$ mice. DKO mice had markedly impaired tooth eruption. Bone mineral density (BMD) was increased 21% to 33% in 4- to 6-week-old DKO mice at all sites when measured by dual-energy X-ray absorptiometry (DXA) and serum cross-linked C-telopeptide (CTx) was reduced by 52%. The amount of metaphyseal trabecular bone was markedly increased in DKO mice, but the cortices were very thin. Spinal trabecular bone mass was increased. Histomorphometry revealed significant reductions in both osteoclast and osteoblast number and function in 4- to 6-week-old DKO animals. In 14- to 16-week-old animals, osteoclast number was increased, although bone density was further increased. DKO osteoclasts had severely impaired actin ring formation, an impaired ability to generate acid, and reduced resorptive activity in vitro. In addition, their life span ex vivo was reduced. DKO osteoblasts expressed normal differentiation markers except for the expression of osterix, which was reduced. The DKO osteoblasts mineralized normally in vitro, indicating that the in vivo defect in osteoblast function was not cell autonomous. Confocal

Address correspondence to: Karl L Insogna, MD, Department of Internal Medicine, Section of Endocrinology, PO Box 208020, Yale School of Medicine, 333 Cedar Street, New Haven, CT 06520-8020, USA. karl.insogna@yale.edu.

Additional Supporting Information may be found in the online version of this article.

**Disclosures**

All authors state that they have no conflicts of interest.

Authors' roles: KLI designed the studies reported here. MZ, B-hS, KS, CS, NT, SLD, LMT-L, EN, JPP, RSW, and SMT assisted with the design of the studies and executed them. KLI, SLD, RSW, and SMT interpreted the data. KLI, SLD, RSW and MZ wrote the manuscript All authors agree to the integrity of the work included in this manuscript and approved the final version of the manuscript.

imaging demonstrated focal disruption of the osteocytic dendritic network in DKO cortical bone. Despite these changes, DKO animals had a normal response to treatment with once-daily parathyroid hormone (PTH). We conclude that Rac1 and Rac2 have critical roles in skeletal metabolism.

### Keywords

RAC1; RAC2; OSTEOCLASTS; OSTEOCYTES

## Introduction

Rac has a central role in regulating cytoskeletal remodeling.[1] Osteoclasts are highly motile, and the role of Rac in these cells has been extensively studied in vitro.[2–4]Rac GTPases are activated by guanine nucleotide exchange factors (GEFs) and in osteoclasts, DOCK5 and Vav3 both serve as GEFs for Rac1.[5–7]Vav3 is activated downstream of c-fms, the receptor for CSF1, a growth factor with important roles in osteoclasts.[7–9]C-fms is highly expressed on mature osteoclasts, and CSF1 induces motility in osteoclasts and activates Rac1 in these cells.[7–9]In addition, $Rac2^{-/-}$ osteoclasts are unable to migrate toward a point source of CSF1.[9]Interestingly, CSF1 is the principal colony-stimulating activity released by osteoblasts in response to parathyroid hormone (PTH).[10]

The roles of Rac1 and Rac2 in osteoclasts have also been studied in vivo. The global Rac1 knock-out mouse is embryonic lethal, so targeted deletion of this molecule is required to study its biology in vivo.[11]Sixteen-week-old mice in which Rac1 has been deleted in cells of the granulocyte and monocyte/macrophage lineages, which include osteoclast precursors, have a 30% increase in bone mass.[12]$Rac2^{-/-}$ mice have an increase in cortical thickness, a reduction in cortical porosity, and an increase in trabecular bone mass in male but not in female mice.[9]These latter changes were observed despite increased numbers of osteoclasts in vivo. Authentic osteoclasts isolated from $Rac2^{-/-}$ mice had impaired actin ring formation and reduced basal rates of bone resorption.[9]The genetic absence of Rac2 in osteoclasts is associated with a more than two-fold increase in the expression of Rac1 protein in these cells, suggesting functional compensation between these two isoforms.[9]

PTH is the only approved anabolic therapy. Interestingly, $Rac2^{-/-}$ mice have an augmented anabolic response to PTH.[13]To determine if there was redundancy in the actions of Rac1 and Rac2 in mature osteoclasts and to study the response to PTH in their absence, we deleted Rac1 and Rac2 in mature osteoclasts. We characterized their skeletal and cellular phenotype and determined their response to an anabolic PTH treatment regimen.

## Materials and Methods

### Materials

Human CSF1 was from Genetics Institute (Cambridge, MA, USA). PTH was from BACHEM (Torrance, CA, USA). Alexa Fluor 488 phalloidin was from Molecular Probes (Eugene, OR, USA). OsteoAssay Human Bone Plates were from Lonza (Walkersville, MD, USA). Acridine orange staining solution was from Immunochemistry (Bloomington, MN,

USA). TUNEL assays were performed using a commercially available kit (Click-iT TUNEL assay, Life Technologies, Grand Island, NY, USA).

### PTH treatment protocols

Twelve wild-type (WT) mice and 10 mice with deletion of both Rac1 and Rac2 in mature osteoclasts (DKO) were assigned to single daily injections of either vehicle or 80 ng/g BW of (1–34) hPTH for 29 days as previously reported.[13] The four treatment groups were vehicle/DKO, PTH/DKO, vehicle/WT, and PTH/WT. Bone density was measured by DXA before and after 29 days of treatment.

### Bone density measurements

In vivo bone density measurements using a PIXImus densitometer and ex vivo micro–computed tomography were performed as previously reported.[14]

### Bone histomorphometry

Histomorphometry was performed as previously reported[15–17] in a ~2.5 $mm^2$ area of distal femoral cancellous bone containing only secondary spongiosa and located 0.5 to 2.5 mm proximal to the epiphyseal growth cartilage. Accepted nomenclature was used to report results.[18,19]

### Phalloidin staining of osteoclasts

Mature osteoclasts were freshly isolated from DKO and CTRL mice and the actin cytoskeleton visualized using Alexa Fluor 488 as previously reported.[7,9,20]

### Bone resorption assay

The osteoclast resorption assay was performed using the OsteoAssay Human Bone plate. These plates are coated with human bone chips, and resorption is quantified by measuring cross-linked C-telopeptide (CTx) released into the media. Osteoclast-like cells (OCLs) were cultured on the human bone plate for 6 days. The CTx concentration in the media from days 3 to 6 of culture was quantified.

### Phalloidin staining and confocal imaging of osteocyte morphology

Femurs and humeri from 10–17-week-old CTRL and DKO mice were fixed in paraformaldehyde, decalcified in 14% EDTA, equilibrated in 15% and then 30% sucrose in PBS, and embedded in OCT. Cryosections (50 μm) were cut from the midshaft of the bones. The sections were incubated overnight at 4°C in PBS + 1% donkey serum + 0.05% NaN3, then stained en bloc with 0.165 μM Alexa Fluor 488 phalloidin overnight at 4°C. The sections were washed with PBS, counterstained in 4 ug/mL DAPI for 30 minutes at room temperature, washed in PBS, and mounted. Z series confocal images were acquired on a Leica (Buffalo Grove, IL, USA) TCS Sp5 II confocal microscope.

Additional Methods are provided in the Supplemental Materials.

### Statistical analyses

Statistical analyses were performed using GraphPad Prism version 5.0c (GraphPad Software Inc., San Diego, CA, USA). Two-tailed *t* tests or Fisher's exact test were used where appropriate. A $p$ value <0.05 was considered significant.

## Results

### Rac1-OC$^{-/-}$ mice have normal bone mass at 9 weeks of age

When LysM-Cre is used to delete Rac1 in vivo in cells of the granulocyte and monocyte/macrophage lineages, Wang and colleagues reported an increase in bone mass at 16 weeks of age.[12]In the current study, in which cathepsin-Cre was used to delete Rac1 in mature osteoclasts, there was no change in bone mass in 9-week-old Rac1-OC$^{-/-}$ mice (Supplemental Fig. S1). The Rac1-OC$^{-/-}$ mice were not studied at older ages. Sex-specific bone density data are provided in Supplemental Fig. S2).

### DKO mice have impaired tooth development

Mice with deletion of both Rac1 and Rac2 only in osteoclasts (DKO mice) were engineered as described in the Supplemental Methods and Supplemental Fig. S3. To quantify expression of the two Rac isoforms in DKO mice, osteoclast-like cells were generated from CTRL and DKO animals and RNA isolated from these cultures to use as a template for qPCR. DKO mice should only have Rac1 deleted in mature osteoclasts; however, one cannot isolate authentic mature osteoclasts in sufficient numbers to perform qPCR, so, as just noted, marrow cultures were used. In these cultures, approximately 80% of the cells are mature osteoclasts. As shown in Supplemental Fig. S4, by qPCR there was a 50% reduction in expression of Rac1 and, as expected, no expression of Rac2.Weuseda PBD pull-down assay to assess the amount of activated Rac1 present in the DKO osteoclasts. As shown in Supplemental Fig. S5, there was virtually no activated Rac1 present in the DKO osteoclast cultures. As shown in Fig. 1A, at 3 weeks of age, all DKO mice were toothless. By 4 weeks of age, a few DKO mice evidenced eruption of their upper incisors. However, no DKO mice ever developed lower incisors. At ages 14 to 16 weeks, DKO and CTRL mice had identical body weights (22 ± 1 versus 22 ± 1 g;$n$ = 10 versus 12; DKO versus CTRL).

### Serum biochemistries are normal, but serum CTx is lower in DKO mice

Serum calcium and phosphorous were not statistically significantly different in DKO and CTRL animals. Serum PTH tended to be higher in the DKO animals, but this change was not statistically significant (Supplemental Table S1). In contrast, mean serum CTx was less than half the value observed in CTRL animals (29.6 ± 4.5 versus 62.3 ± 10.4 ng/mL; DKO versus CTRL). The sex-specific changes in serum CTx are summarized in Supplemental Fig. S6.

### DKO mice have higher bone density with increased trabecular bone but thin cortices

Compared with littermate CTRLs, 4- to 6-week-old DKO mice had significantly higher bone density when measured by PIXImus at all sites (Fig. 1C). Spine bone density was increased by 33% (0.0643 ± 0.0040 versus 0.0482 ± 0.0019 g/cm$^2$; DKO versus CTRL). Femur bone

density was 21% higher (0.0753 ± 0.0047 versus 0.0623 ± 0.0028 g/cm$^2$; DKO versus CTRL), and total body bone density was higher by 24% (0.0544 ± 0.0024 versus 0.0440 ± 0.0017 g/cm$^2$; DKO versus CTRL). The changes were even more pronounced in 14- to 16-week-old animals (Fig. 1D). The sex-specific changes in bone mineral density (BMD) are summarized in Supplemental Fig. S7.

There was a marked increase in the extent of trabecular bone in femurs from DKO mice (Fig. 1B, left two panels), which was present throughout the entire medullary cavity and well into the diaphysis. In contrast, the cortices were thin in the DKO animals (Fig. 1B, right two panels). When quantified by micro-CT, cortical bone volume was reduced by 47% in the DKO animals (46 ± 1.2 versus 87 ± 1.5%; DKO versus CTL). The periosteal and endosteal diameters were significantly greater in the DKO animals (Supplemental Table S2). Micro-CT analyses of the 3rd lumbar vertebrae showed a marked increase in trabecular bone volume with an increase in trabecular number and a reduction in trabecular thickness (Supplemental Table S3).

### Femurs of DKO mice have altered biomechanics

The four-point bending tests revealed that the presence of trabecular bone in the femoral diaphysis altered the biomechanics of the DKO femurs. The stiffness of DKO femurs was 33% greater than the littermate CTRL femurs. The most striking difference in whole bone properties was a 104% increase in maximum load and a 188% increase in work to fracture (total work) of the DKO femurs compared with littermate CTRLs (Supplemental Table S4). These results indicated that despite thinner cortices, the presence of trabecular bone in the femoral diaphysis increased the stiffness and strength of the DKO femurs. The sex-specific changes in biomechanics are shown in Supplemental Table S5.

### DKO mice have altered numbers and activity of osteoblasts and osteoclasts in bone

To further evaluate the cellular bases for the changes observed in bone mass, histomorphometry was performed (Table 1). Four-week-old DKO mice showed significant reductions in osteoid surface, osteoblast surface, as well as the number of osteoblasts per osteoid perimeter. Osteoclast surface per bone surface as well as the number of osteoclasts per bone perimeter were also significantly reduced in the DKO animals. Bone volume per tissue volume (BV/TV) was not different in the two groups because trabecular bone density in the femur was not different in the region just below the growth plate where histomorphometric measurements are made, but the extent of trabecular bone mass was obviously increased (Fig. 1B). However, as noted, in the spine trabecular bone volume was significantly increased (Supplemental Table S3). Although the number of osteoclasts was significantly reduced in the 4-week-old DKO animals, this finding was reversed in older animals. Thus, at 14 to 16 weeks of age, osteoclast number was actually increased (NOc/BPm 3.81 ± 1.1 versus 1.27 ± 0.20, $p = 0.03$; OcS/BS 13.38 ± 3.5 versus 4.20 ± 0.5, p = 0.02; NOc/TAR 63.46 ± 11.9 versus 10.63 ± 1.7, $p < 0.001$; DKO versus CTRL; see vehicle-treated groups in Table 2). The sex-specific differences in histomorphometry are shown in Supplemental Table S6.

### DKO osteoclasts have a shortened life span in vitro

Details of how mature osteoclasts were prepared for this experiment are included in the Supplemental Methods. A total of 31 CTRL and 21 DKO authentic osteoclasts were directly isolated from neonatal bone and studied in 3 separate experiments. Cells were isolated from 3 CTRL and 3 DKO animals in each experiment. When cultured, ex vivo mature osteoclasts freshly isolated from DKO animals had a significantly higher proportion of TUNEL-positive cells at 10 hours than did CTRL cells. Fifteen of 21 DKO osteoclasts stained positive compared with 10 of 31 CTRL cells ($p = 0.01$ by Fisher's exact test; Supplemental Fig. S8).

### DKO osteoclasts generate less acid, fail to form actin rings, and have markedly reduced resorptive activity in vitro

To determine if a defect in osteoclast acidification was responsible for their impaired resorptive activity, osteoclasts freshly isolated from DKO animals were stained with acridine orange and the number of orange-stained cells compared with the number of orange-stained CTRL osteoclasts. Acridine orange has been extensively used to evaluate acidification in osteoclasts.[21–24]As shown in Fig. 2A, acridine orange staining in DKO osteoclasts was diminished compared with CTRL cells. In addition, DKO osteoclasts had markedly impaired actin ring formation (Fig. 2B). DKO osteoclasts also had impaired resorptive activity when assayed on human bone particles (Fig. 2C).

### Expression of differentiation markers and mineralizing capacity of DKO osteoblasts

The findings of reduced osteoblast number and function in vivo in the DKO animals is surprising. Rac1 expression in osteoblasts should not be affected by deletion of this isoform in osteoclasts. The global deletion of Rac2 should not affect osteoblasts because these cells do not express Rac2 (Supplemental Fig. S9). Rac2 is only expressed in hematopoietic tissue.[25]Further, we have reported that osteoblast function is normal in vivo in $Rac2^{-/-}$ mice.[9]To determine if there was a cell-autonomous defect in DKO osteoblasts, CTRL and DKO osteoblasts were isolated, cultured to confluence, and the level of expression of key osteoblasts markers assessed by qPCR. As shown in Supplemental Fig. S10B, the levels of expression of Runx2, collagen 1α1, and osteocalcin were indistinguishable in the two cells types, although osterix was lower in the DKO mice. In vitro mineralization occurred to the same extent in osteoblasts cultured from DKO mice and osteoblasts prepared from CTRL animals (Supplemental Fig. S11). The calcium and phosphate content in the mineralized cell layers was not significantly different in DKO and CTRL cultures (calcium 3.4 ± 0.6 versus 2.2 ± 0.6, DKO versus CTRL; phosphorous 2.3 ± 0.4 versus 1.6 ± 0.3, DKO versus CTRL). Interestingly, although osteoblast function was similar to CTRLs in vitro, the amount of collagen transcript expressed in the bone of DKO animals was significantly reduced (Supplemental Fig. S10A), consistent with the finding of a reduced number of osteoblasts in vivo.

### DKO mice have a normal response to an anabolic PTH regimen

As shown in Fig. 3, bone density assessed by dual-energy X-ray absorptiometry (DXA) increased to a comparable extent in DKO and WT animals after 29 days of treatment with 80 ng/kg/d of (1–34) hPTH. For example, in the femur, BMD increased by 18.2 ± 3.5% in the

PTH-treated DKO animals and with vehicle treatment by 5.6 ± 2.5% for a net difference of ± 12.6%. In WT animals, PTH treatment led to a 20.8 ± 2.3% increase in femur BMD, whereas vehicle treatment caused an 11.7±1.7% increase for a net difference + 9.1%. At the spine, the average difference in the percent increase in BMD between PTH-treated and vehicle-treated DKO animals was + 8.5%, whereas in WT animals, it was + 2.3%. In the total body, the values were 6.9% and 4.3%, DKO and WT, respectively. In absolute terms, spinal BMD increased by 156 ± 30 $g/cm^2 \times 10^{-4}$ in the DKO animals and by 71 ± 12$g/cm^2 \times 10^{-4}$ in WT after PTH treatment. In the femur, the mean values were 204 ± 30 $g/cm^2 \times 10^{-4}$ in the DKO animals and 141 ± 13$g/cm^2 \times 10^{-4}$ in WT animals. For the total body, the values were 105 ± 20$g/cm^2 \times 10^4$ versus 61 ± 5 $g/cm^2 \times 10^{-4}$, respectively. There was no difference based on genotype for the change in BMD in vehicle-treated DKO animals and vehicle-treated WT animals (Supplemental Table S7). Supplemental Table S8 summarizes the sex-specific changes in bone density in response to PTH.

With PTH treatment, osteoblast parameters tended to increase in both the DKO and WT animals, although, because of the small numbers of animals studied, these trends were not significant. However, there was a qualitative difference in the PTH-induced changes in parameters of osteoclast function. In particular, OcS/BS and NOc/BPm tended to increase in the WT animals and the NOc/TAR increased significantly. In contrast and surprisingly, these same parameters did not change with PTH treatment in the DKO animals and, in fact, tended to decrease (Table 2). The sex-specific histomorphometric changes in response to PTH are summarized in Supplemental Table S9. One explanation for the failure of osteoclast number to increase with PTH treatment in the DKO animals could be a change in the level of expression of receptor activator of NF-κB ligand (RANKL). However, as shown in Supplemental Fig. S12, tissue levels of RANKL were higher in both vehicle and PTH-treated DKO mice. Dynamic histomorphometric data in vehicle and PTH-treated DKO and WT animals are presented in Supplemental Table S10. Both groups of animals showed increases in mineral apposition rate and bone formation rate per bone surface, although the changes were only significant in the CRTLs. The sex-specific effects of PTH treatment on dynamic histomorphometric measurements are shown in Supplemental Table S11.

## Expression levels of sclerostin, LRP4, and SPHK1 are altered in DKO mice

Because osteoblast function was impaired in vivo but not in vitro in DKO mice, this suggested that a paracrine or endocrine inhibitor of osteoblast activity was the basis for this finding. Two paracrine signaling molecules that regulate osteoblast activity and for which compelling supportive in vivo evidence exists are sclerostin and sphingosine-1-phosphate, the former a potent inhibitor of bone formation and the latter an osteoclast-derived paracrine anabolic signal for osteoblasts.[26–28] We initially examined serum levels of sclerostin in DKO animals and found that they were significantly elevated (1727 ± 137 versus 984 ± 112 pg/mL, DKO versus CTRL, $p = 0.002$, $n = 6$ for both groups). However, it has recently been reported that LRP4 tethers sclerostin in bone.[29] When LRP4 is deleted in vivo, circulating levels of sclerostin rise, but bone formation is not suppressed, suggesting that local sclerostin in bone and not circulating sclerostin is important in controlling bone formation. We, therefore, examined SOST and LRP4 transcript expression and LRP4 protein levels in DKO cortical bone and found that expression of both SOST and LRP4 were markedly lower than

in CTRLs (Supplemental Fig. S13A). By Western blot, the level of LRP4 protein was also found to be significantly lower in the DKO animals (Supplemental Fig. S13B). The reduced expression of LRP4 likely explains the high levels of serum sclerostin in our animals but may not explain the suppressed bone formation. Another paracrine signaling pathway that is more directly related to osteoclasts is the sphingosine-1-phosphate (S1P) pathway recently elucidated in two studies, both of which concluded that increased production of S1P by osteoclasts controls bone formation in vivo.[28,30] Two molecular mechanisms in osteoclasts have been reported to regulate S1P production. In one, increased expression of the rate-limiting enzyme for S1P synthesis, SPHK1, is responsible for the increase in S1P production and in the other, increased expression of the cellular S1P exporter, SPNS2, is increased.[28,30] We examined expression of both of these in osteoclasts isolated from DKO mice and found that SPHK1 expression was decreased, whereas expression of SPNS2 was unaltered, suggesting that reduced production of S1P may in part explain the reduced rate of bone formation in the DKO animals (Supplemental Fig. S14).

Serum levels of sclerostin did fall to a greater extent with PTH treatment in the DKO animals than the WT animals (Supplemental Fig. S15), but for the reasons just noted, it is not clear if this played a role in the response to an anabolic PTH regimen in the DKO animals. The sex-specific changes in circulating sclerostin at day 29 of treatment are summarized in Supplemental Fig. S16).

## Focal disruption of the osteocytic network in DKO mice

The findings in DKO animals of elevated serum sclerostin and reduced transcripts in bone of SOST and LRP4 raised the possibility of an abnormality in osteocytes. Using phalloidin staining of decalcified femoral and humeral cortical bone slices and confocal microscopy, the osteocytes in DKO and CTRL animals were imaged (Fig. 4A, B). The DKO mice had large areas of abnormal-appearing bone in the cortices (Figs. 4A, B, right third panelin each upper row, red arrows, and third panel in each lower row, red arrows). The CTRL animals showed little to no evidence of this (Fig. 4A, B, upper first panel in each top row). Under higher magnification (Fig.4A, B, third panel in each upper and lower row), there appeared to be areas of discontinuity in the DKO cortex with seams/interfaces separating areas of bone. Imaging of the osteocytes in these areas revealed discontinuities in the osteocyte network and isolated islands of osteocytes that did not connect across the interfaces (Fig. 4A, B, upper and lower rows, last panel). In CTRL bone, osteocytes showed a highly regular organization with extensive interconnectivity between osteocytes (Figs. 4A, B, upper and lower rows, second panel). The anatomical region of each bone analyzed was precisely defined (Supplemental Figs. S17 and S18), so the differences observed are not the result of analyses conducted in different regions of the CTRL and DKO bone. In contrast to the findings in the DKO mice, the osteocyte network was normal in the $Rac2^{-/-}$ mice (Supplemental Fig. S19).

To determine if this disrupted osteocytic network was associated with changes in the organization of collagen in bone, collagen architecture was examined after decalcification using polarized light microscopy. As shown in Supplemental Fig. S20, both DKO and CTRL bones demonstrated lamellar collagen with no evidence of abnormal collagen organization.

## Discussion

The findings in the present study combined with earlier work by Itokawa and colleagues and Wang and colleagues establish that there is significant functional overlap between Rac1 and Rac2 in osteoclasts.[9,12]Selective deletion of each leads to relatively mild phenotypes in vivo, whereas, as the current study demonstrates, the deletion of both in mature osteoclasts leads to marked impairment in the function of these cells and a severe osteopetrotic phenotype. In addition, the DKO animals evidenced a surprising reduction in the number of osteoblasts in vivo. Despite increased trabecular bone mass, the cortices of the DKO animals were thinned. Cortical histology similar to that found in the DKO animals appears to be present in another osteopetrotic animal, the c-src knock-out mouse.[31]In contrast, the cortex appears relatively normal in two osteopetrotic mouse models in which osteoclasts are absent, namely the op/op mouse and the c-fos knock-out mouse.[32,33]

DKO osteoclasts have severely impaired resorbing capacity and a shortened life span in vitro. This latter finding is consistent with the relative paucity of osteoclasts found in vivo in young animals, although as animals age, the number of osteoclasts present in bone actually increased, which might reflect a compensatory response to the resorptive defect in these cells. Despite this, the osteopetrotic phenotype worsened. The cellular basis for the resorptive defect in the DKO osteoclasts is likely the result of a failure of actin ring formation and a reduced life span. The defective actin dynamics in the DKO osteoclasts is consistent with the known roles of Rac1 and Rac2 in cytoskeletal remodeling and chemotaxis.[7,9]Cellular acidification was also impaired in DKO osteoclasts, which likely contributed to the defect in resorptive activity.

The reduction in osteoblast number in vivo in the DKO mice was not cell-autonomous because DKO osteoblasts had a largely normal molecular profile, although levels of osterix were reduced. Functionally, the DKO osteoblasts appeared unimpaired because they mineralized normally ex vivo. It is unlikely that off-target deletion of Rac1 in osteocytes explains this change because cathepsin K is not expressed in osteocytes except during pregnancy/lactation.[34]It is unlikely that impaired osteoclast resorptive activity explains the reduction of osteoblast number because there are at least two osteopetrotic mouse models in which osteoclast resorptive function is impaired but osteoblast activity is increased, the cathepsin K knock-out mouse[30]and c-src knock-out mouse.[35]We are uncertain what explains the reduced numbers of osteoblasts in vivo, but as noted in Results, a reduction in sphingosine-1-phosphate production by the DKO osteoclasts may be playing a role. We also found evidence for a dysfunction of osteocytes with a disruption of the osteocyte network, reduced expression of LRP4, and increased circulating levels of sclerostin. Although there are no previous reports of circulating sclerostin levels in other osteopetrotic models, in the Hyp mouse, another animal model where bone microarchitecture is disrupted, sclerostin transcript expression in bone is elevated.[36]The basis for the disrupted osteocyte network in the DKO mice is most likely secondary to a failure of normal bone modeling and remodeling. This is, in turn, owing to the defect in osteoclast resorptive activity found in the DKO osteoclasts. The failure of bone remodeling leads to an abnormal bone microarchitecture as illustrated in Fig. 4 that leads to a disruption of the osteocyte network, which may contribute to the dysregulated osteocyte function. Thus, it is the resorptive defect

in the DKO osteoclasts that ultimately results in osteocyte dysfunction, not directly but rather indirectly by affecting bone microarchitecture.

Wang and colleagues used LysM cre transgenic mice to delete Rac1 in cells of the leukocyte-monocyte lineage and then bred those animals to $Rac2^{-/-}$ mice.[12]These mice had normal tooth eruption but increased bone density and the marrow of these animals evidenced impaired osteoclastogenic capacity. Croke and colleagues also reported an osteopetrotic phenotype in animals engineered in the same way, and, like Wang and colleagues, Croke and colleagues reported normal tooth eruption in their animals.[37]Croke and colleagues also found impaired osteoclastogenic potential in the marrow of these mice. Osteoclast-like cells generated in vitro did not form actin rings normally and evidenced poor resorptive activity.[37]In these models, Rac1 is deleted early in the osteoclast lineage as well as in macrophages and leukocytes. Consequently, studies with these animals do not address the role of the two Rac isoforms just in differentiated osteoclasts. Further, the abnormalities reported in these two previous studies could reflect effects on other cell lineages such as neutrophils and mature macrophages. In contrast, in the present study by using the cathepsin K cre mouse, Rac1 is only deleted in osteoclasts excluding a contribution of other cell lineages to our findings. In their report, Croke and colleagues also describe animals generated in a manner similar to ours, using the cathepsin K cre knock-in mouse to delete Rac1 and observed an osteopetrotic phenotype and impaired tooth eruption.[37]The reason that both Croke and colleagues and Wang and colleagues did not observe impaired tooth eruption using the LysM cre to delete Rac1, while this phenotype was observed when cathepsin K cre was used to delete Rac1, may be because cathepsin K cre more completely deletes Rac 1.[37]Surprisingly, Croke and colleagues reported that in the double knock-out mice generated using cathepsin K cre to delete Rac1, actin ring formation and resorption were normal in osteoclast-like cells differentiated in vitro. This is difficult to reconcile with the osteopetrotic phenotype of these animals. Our findings of a marked defect in actin ring formation in authentic, freshly isolated mature osteoclasts is in keeping with our in vivo osteopetrotic phenotype and the lower serum CTx values in the DKO animals. We found markedly impaired resorptive activity of osteoclast-like cells differentiated in vitro, again consistent with the in vivo phenotype. None of the prior reports have provided histomorphometric data, so it is unclear if the defect we found in osteoblast function in vivo is found in these other models. Biomechanical data were also not provided in any of the prior studies. We also showed for the first time that DKO osteoclasts have a reduced ability to generate acid.

It has recently been reported that in addition to its expression in osteoclasts, cathepsin K is endogenously expressed in an ovary and testis.[38,39]We confirmed expression of our transgene in testis, but unlike Winkeler and colleagues,[38,39]we did not see expression in the gametes (Supplemental Methods and Supplemental Fig. S21). Because global deletion of Rac1 is embryonic lethal,[11]if Rac1 was expressed in the gametes, it would lead to embryonic lethality early in our breeding strategy, which we did not observe.

Despite the marked cellular abnormalities in the DKO animals, bone density increased to the same if not greater extent than WT animals when given single daily injections of PTH. The reasons for this surprising finding are not entirely clear. Unlike in WT animals, in DKO

animals there was no increase in osteoclast number with PTH treatment. In fact, osteoclast number declined slightly. Although these cells are dysfunctional, a decline in osteoclast number could uncouple the anabolic response in favor of formation.

In summary, our data support important nonredundant roles for Rac1 and Rac2 in mature osteoclasts, as well as significant functional overlap between these two. They also highlight the cellular complexity of the anabolic response to PTH. Finally, they raise the possibility that skeletal microarchitecture and impaired osteoclast activity impact normal osteocyte function.

## Supplementary Material

Refer to Web version on PubMed Central for supplementary material.

## Acknowledgments

This work was supported by NIH grants DE12459 and DK45228 (to KLI) and by the Yale Core Center for Musculoskeletal Disorders, which was supported by a P30 Core Center Award from NIAMS (AR46032, PI: KLI). The work was also partially supported by NIH grants P01 AG039355 and S10 RR027668 (to SLD) and by a VA Merit Review Grant from the Office of Research and Development, Department of Veterans Affairs, and the National Institutes of Health (P01-AG13918 to RSW). The Yale Bone Center also supported this work.

## References

1. Etienne-Manneville S, Hall A. Rho GTPases in cell biology. Nature. 2002; 420(6916):629–35. [PubMed: 12478284]
2. Razzouk S, Lieberherr M, Cournot G. Rac-GTPase, osteoclast cytoskeleton and bone resorption. Eur J Cell Biol. 1999; 78(4):249–55. [PubMed: 10350213]
3. Ory S, Munari-Silem Y, Fort P, Jurdic P. Rho and Rac exert antagonistic functions on spreading of macrophage-derived multinucleated cells and are not required for actin fiber formation. J Cell Sci. 2000; 113(Pt 7):1177–88. [PubMed: 10704369]
4. Fukuda A, Hikita A, Wakeyama H, et al. Regulation of osteoclast apoptosis and motility by small GTPase binding protein Rac1. J Bone Miner Res. 2005; 20(12):2245–53. [PubMed: 16294277]
5. Vives V, Laurin M, Cres G, et al. The Rac1 exchange factor Dock5 is essential for bone resorption by osteoclasts. J Bone Miner Res. 2011; 26(5):1099–110. [PubMed: 21542010]
6. Faccio R, Teitelbaum SL, Fujikawa K, et al. Vav3 regulates osteoclast function and bone mass. Nat Med. 2005; 11(3):284–90. [PubMed: 15711558]
7. Sakai H, Chen Y, Itokawa T, Yu KP, Zhu ML, Insogna K. Activated c-Fms recruits Vav and Rac during CSF-1-induced cytoskeletal remodeling and spreading in osteoclasts. Bone. 2006; 39(6): 1290–301. [PubMed: 16950670]
8. Grey A, Chen Y, Paliwal I, Carlberg K, Insogna K. Evidence for a functional association between phosphatidylinositol 3-kinase and c-src in the spreading response of osteoclasts to colony-stimulating factor-1. Endocrinology. 2000; 141(6):2129–38. [PubMed: 10830300]
9. Itokowa T, Zhu M-L, Troiano N, Bian J, Kawano T, Insogna K. Osteoclasts lacking rac2 have defective chemotaxis and resorptive activity. Calcif Tissue Int. 2011; 88(1):75–86. [PubMed: 21110188]
10. Weir EC, Horowitz MC, Baron R, Centrella M, Kacinski BM, Insogna KL. Macrophage colony-stimulating factor release and receptor expression in bone cells. J Bone Miner Res. 1993; 8(12): 1507–18. [PubMed: 8304053]
11. Glogauer M, Marchal CC, Zhu F, et al. Rac1 deletion in mouse neutrophils has selective effects on neutrophil functions. J Immunol. 2003; 170(11):5652–7. [PubMed: 12759446]

12. Wang Y, Lebowitz D, Sun C, Thang H, Grynpas MD, Glogauer M. Identifying the relative contributions of rac1 and rac2 to osteoclastogenesis. J Bone Miner Res. 2008; 23(2):260–70. [PubMed: 17922611]
13. Kawano T, Troiano N, Adams DJ, Wu JJ, Sun BH, Insogna K. The anabolic response to parathyroid hormone is augmented in Rac2 knockout mice. Endocrinology. 2008; 149(8):4009–15. [PubMed: 18467443]
14. Kawano T, Zhu M, Troiano N, et al. LIM kinase 1 deficient mice have reduced bone mass. Bone. 2013; 52(1):70–82. [PubMed: 23017662]
15. Insogna KL, Stewart AF, Vignery AM, et al. Biochemical and histomorphometric characterization of a rat model for humoral hypercalcemia of malignancy. Endocrinology. 1984; 114(3):888–96. [PubMed: 6546543]
16. Knopp E, Troiano N, Bouxsein M, et al. The effect of aging on the skeletal response to intermittent treatment with parathyroid hormone. Endocrinology. 2005; 146(4):1983–90. [PubMed: 15618351]
17. Yao GQ, Wu JJ, Ovadia S, Troiano N, Sun BH, Insogna K. Targeted overexpression of the two colony-stimulating factor-1 isoforms in osteoblasts differentially affects bone loss in ovariectomized mice. Am J Physiol Endocrinol Metab. 2009; 296(4):E714–20. [PubMed: 19141689]
18. Parfitt AM, Drezner MK, Glorieux FH, et al. Bone histomorphometry: standardization of nomenclature, symbols, and units. Report of the ASBMR Histomorphometry Nomenclature Committee. J Bone Miner Res. 1987; 2(6):595–610. [PubMed: 3455637]
19. Dempster DW, Compston JE, Drezner MK, et al. Standardized nomenclature, symbols, and units for bone histomorphometry: a 2012 update of the report of the ASBMR Histomorphometry Nomenclature Committee. J Bone Miner Res. 2013; 28(1):2–17. [PubMed: 23197339]
20. Insogna KL, Sahni M, Grey AB, et al. Colony-stimulating factor-1 induces cytoskeletal reorganization and c-src-dependent tyrosine phosphorylation of selected cellular proteins in rodent osteoclasts. J Clin Invest. 1997; 100(10):2476–85. [PubMed: 9366562]
21. Karsdal MA, Henriksen K, Sorensen MG, et al. Acidification of the osteoclastic resorption compartment provides insight into the coupling of bone formation to bone resorption. Am J Pathol. 2005; 166(2):467–76. [PubMed: 15681830]
22. Kornak U, Kasper D, Bosl MR, et al. Loss of the ClC-7 chloride channel leads to osteopetrosis in mice and man. Cell. 2001; 104(2):205–15. [PubMed: 11207362]
23. Palokangas H, Mulari M, Vaananen HK. Endocytic pathway from the basal plasma membrane to the ruffled border membrane in bone-resorbing osteoclasts. J Cell Sci. 1997; 110(Pt 15):1767–80. [PubMed: 9264464]
24. Baron R, Neff L, Louvard D, Courtoy PJ. Cell-mediated extracellular acidification and bone resorption: evidence for a low pH in resorbing lacunae and localization of a 100-kD lysosomal membrane protein at the osteoclast ruffled border. J Cell Biol. 1985; 101(6):2210–22. [PubMed: 3905822]
25. Gu Y, Byrne MC, Paranavitana NC, et al. Rac2, a hematopoiesis-specific Rho GTPase, specifically regulates mast cell protease gene expression in bone marrow-derived mast cells. Mol Cell Biol. 2002; 22(21):7645–57. [PubMed: 12370311]
26. Moester MJ, Papapoulos SE, Lowik CW, van Bezooijen RL. Sclerostin: current knowledge and future perspectives. Calcified tissue international. 2010; 87(2):99–107. [PubMed: 20473488]
27. Lotinun S, Kiviranta R, Matsubara T, et al. Osteoclast-specific cathepsin K deletion stimulates S1P-dependent bone formation. J Clin Invest. 2013; 123(2):666–81. [PubMed: 23321671]
28. Keller J, Catala-Lehnen P, Huebner AK, et al. Calcitonin controls bone formation by inhibiting the release of sphingosine 1-phosphate from osteoclasts. Nat Commun. 2014; 5:5215. [PubMed: 25333900]
29. Chang MK, Kramer I, Huber T, et al. Disruption of Lrp4 function by genetic deletion or pharmacological blockade increases bone mass and serum sclerostin levels. Proc Natl Acad Sci USA. 2014; 111(48):E5187–95. [PubMed: 25404300]
30. Lotinun S, Kiviranta R, Matsubara T, et al. Osteoclast-specific cathepsin K deletion stimulates S1P-dependent bone formation. J Clin Invest. 2013; 123(2):666–81. [PubMed: 23321671]

31. Soriano P, Montgomery C, Geske R, Bradley A. Targeted disruption of the *c*-src proto-oncogene leads to osteopetrosis in mice. Cell. 1991; 64(4):693–702. [PubMed: 1997203]
32. Radi ZA, Guzman RE, Bell RR. Increased connective tissue extracellular matrix in the op/op model of osteopetrosis. Pathobiology. 2009; 76(4):199–203. [PubMed: 19571609]
33. Johnson RS, Spiegelman BM, Papaioannou V. Pleiotropic effects of a null mutation in the c-fos proto-oncogene. Cell. 1992; 71(4):577–86. [PubMed: 1423615]
34. Qing H, Ardeshirpour L, Pajevic PD, et al. Demonstration of osteocytic perilacunar/canalicular remodeling in mice during lactation. J Bone Miner Res. 2012; 27(5):1018–29. [PubMed: 22308018]
35. Marzia M, Sims NA, Voit S, et al. Decreased *c*-Src expression enhances osteoblast differentiation and bone formation. J Cell Biol. 2000; 151(2):311–20. [PubMed: 11038178]
36. Atkins GJ, Rowe PS, Lim HP, et al. Sclerostin is a locally acting regulator of late-osteoblast/preosteocyte differentiation and regulates mineralization through a MEPE-ASARM-dependent mechanism. J Bone Miner Res. 2011; 26(7):1425–36. [PubMed: 21312267]
37. Croke M, Ross FP, Korhonen M, Williams DA, Zou W, Teitelbaum SL. Rac deletion in osteoclasts causes severe osteopetrosis. J Cell Sci. 2011; 124(Pt 22):3811–21. [PubMed: 22114304]
38. Yang W, Wang J, Moore DC, et al. Ptpn11 deletion in a novel progenitor causes metachondromatosis by inducing hedgehog signalling. Nature. 2013; 499(7459):491–5. [PubMed: 23863940]
39. Winkeler CL, Kladney RD, Maggi LB Jr, Weber JD. Cathepsin K-Cre causes unexpected germline deletion of genes in mice. PLoS One. 2012; 7(7):e42005. [PubMed: 22860046]

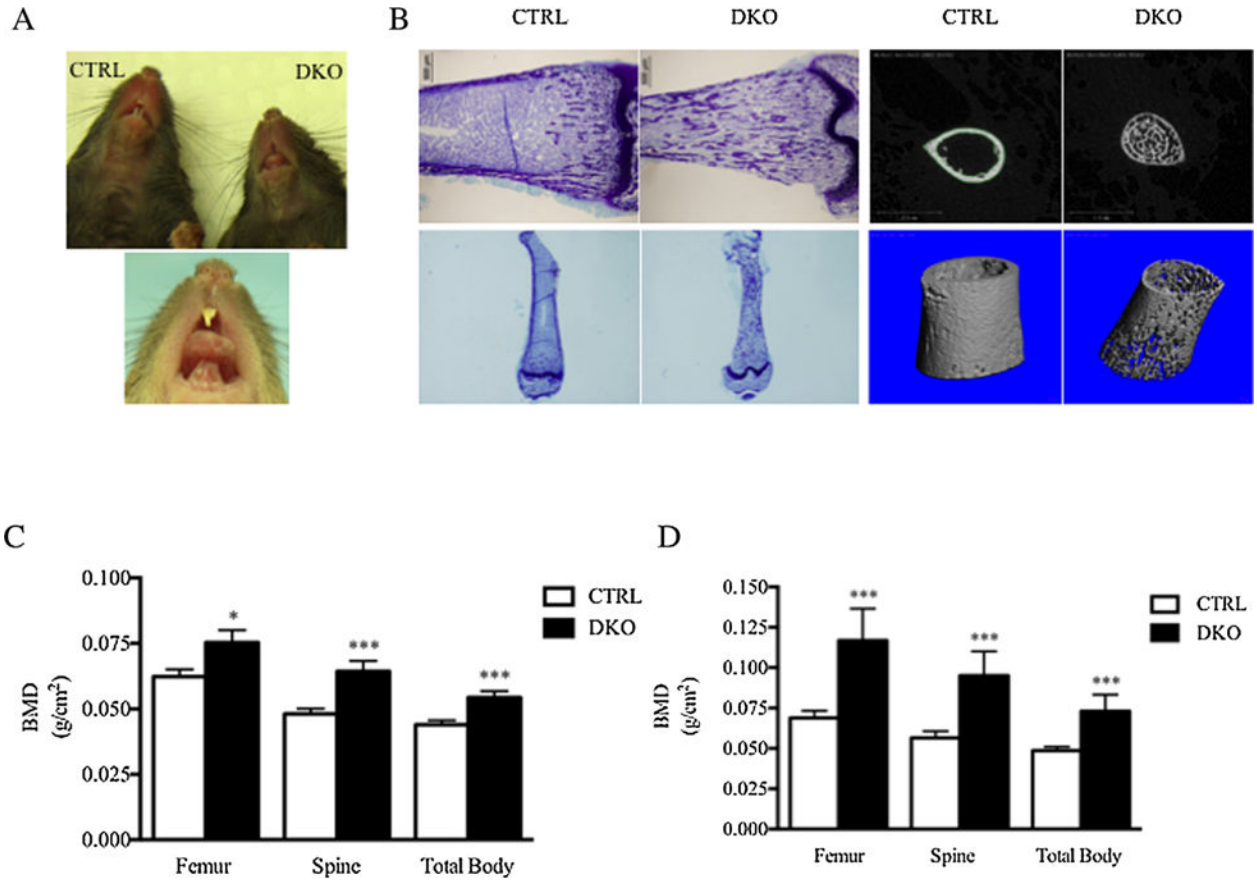


**Fig. 1.**

Impaired tooth eruption and high bone density in DKO mice. (*A*) Upper panel: At age 3 weeks, DKO animals evidenced no tooth eruption. Lower panel: A few animals showed partial eruption of the upper incisors, but no animals ever showed eruption of the lower incisors. (*B*) Left upper two panels: Low-power photomicrograph of toluidine blue-stained distal femurs from 4-week-old DKO and CTRL littermate mice demonstrating persistence of trabecular bone in the femoral metaphysis and diaphysis in DKO mice. Left lower two panels show the same but provide a more complete view of the persistent trabecular bone in the diaphysis. Right four panels: 3-D reconstructions of micro-CT images of diaphyseal bone in 4-week-old DKO mice and littermate CRTLs. Note the persistent trabecular bone in the diaphysis and the marked thinning of the cortex in the DKO mice. (*C*) Bone density by DXA in 4- to 6-week-old DKO and CTRL mice ($n$ = for 29 DKO mice and 34 for CTRL mice). (*D*) Bone density by DXA in 14- to 16-week-old mice ($n$ = 10 for DKO mice and 12 for CTRL mice). *$p < 0.05$, ***$p < 0.001$.

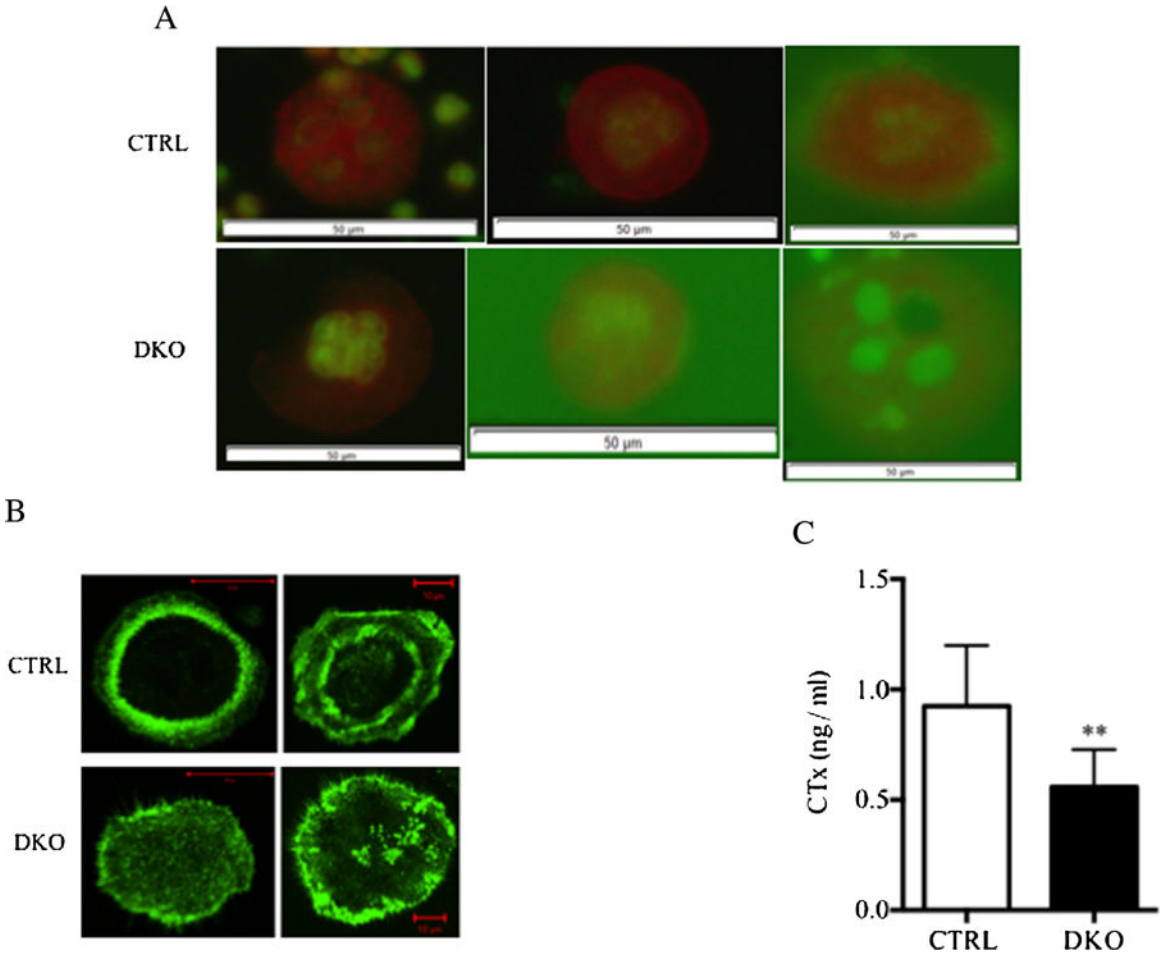


**Fig. 2.**

DKO osteoclasts had reduced acid generation, impaired sealing zone formation, and showed little resorptive activity. (*A*) Acridine orange staining of freshly isolated mature osteoclasts from CTRL (upper panel) and DKO animals (lower panel) plated on OsteoAssay plates. Orange staining reflects acid pH. Nine of nine DKO osteoclasts showed slightly less intense staining with acridine orange, whereas 23 of 23 CTRL cells stained normally. The white scale bar = 50 μM. (*B*) Phalloidin staining of freshly isolated mature osteoclasts from CTRL animals (upper panel) and DKO animals (lower panel) after culturing on FBS-coated glass slides for 6 hours. Actin ring formation is evident in the CTRL cells but not in the DKO cells. A total of 87% (20 of 23) of control cells had normal actin ring formation, whereas only 29% (5 of 17) of DKO osteoclasts were able to form actin rings ($p = 0.0003$ by Fisher's exact test). (*C*) Quantification of the resorptive activity of CTRL and DKO osteoclast-like cells cultured with human bone particles using the OsteoAssay Human bone plate. CTx was measured in the conditioned media from days 3 to 6 of culture ($n = 8$ for each determination). **$p < 0.001$.

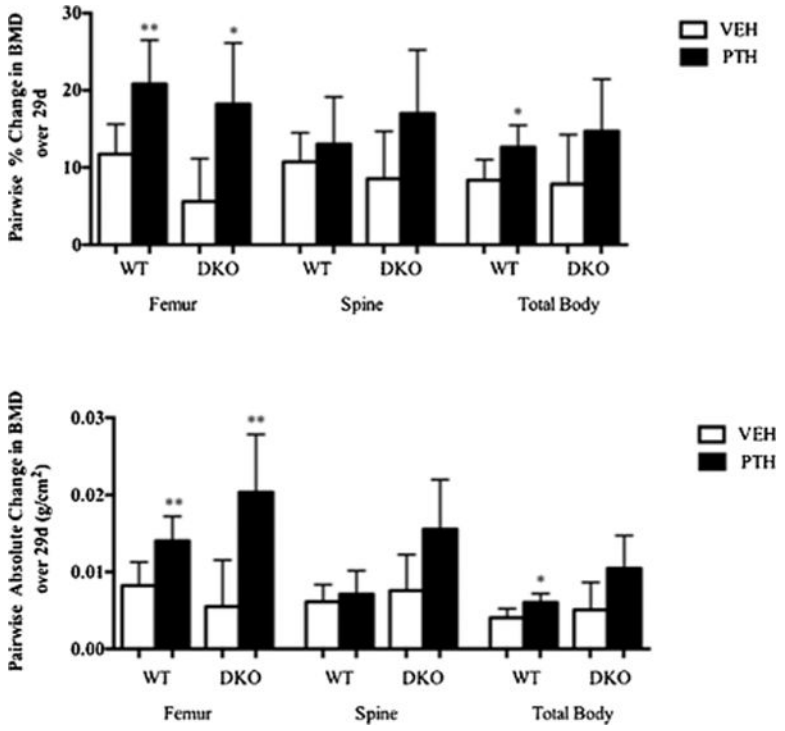


**Fig. 3.**

Changes in BMD in DKO animals treated with an anabolic PTH regimen. Upper panel: Percent change in spine, femur, and total BMD by DXA in WT (open bars) and DKO animals (black bars). Lower panel: Absolute change in spine, femur, and total BMD by DXA in WT (open bars) and DKO animals (black bars).The animals were 18 weeks old ($n$ = 6 for WT-VEH and 6 for WT-PTH; $n$ = 5 for DKO-VEH and 5 for DKO-PTH). *$p$<0.05; **$p$<0.01.

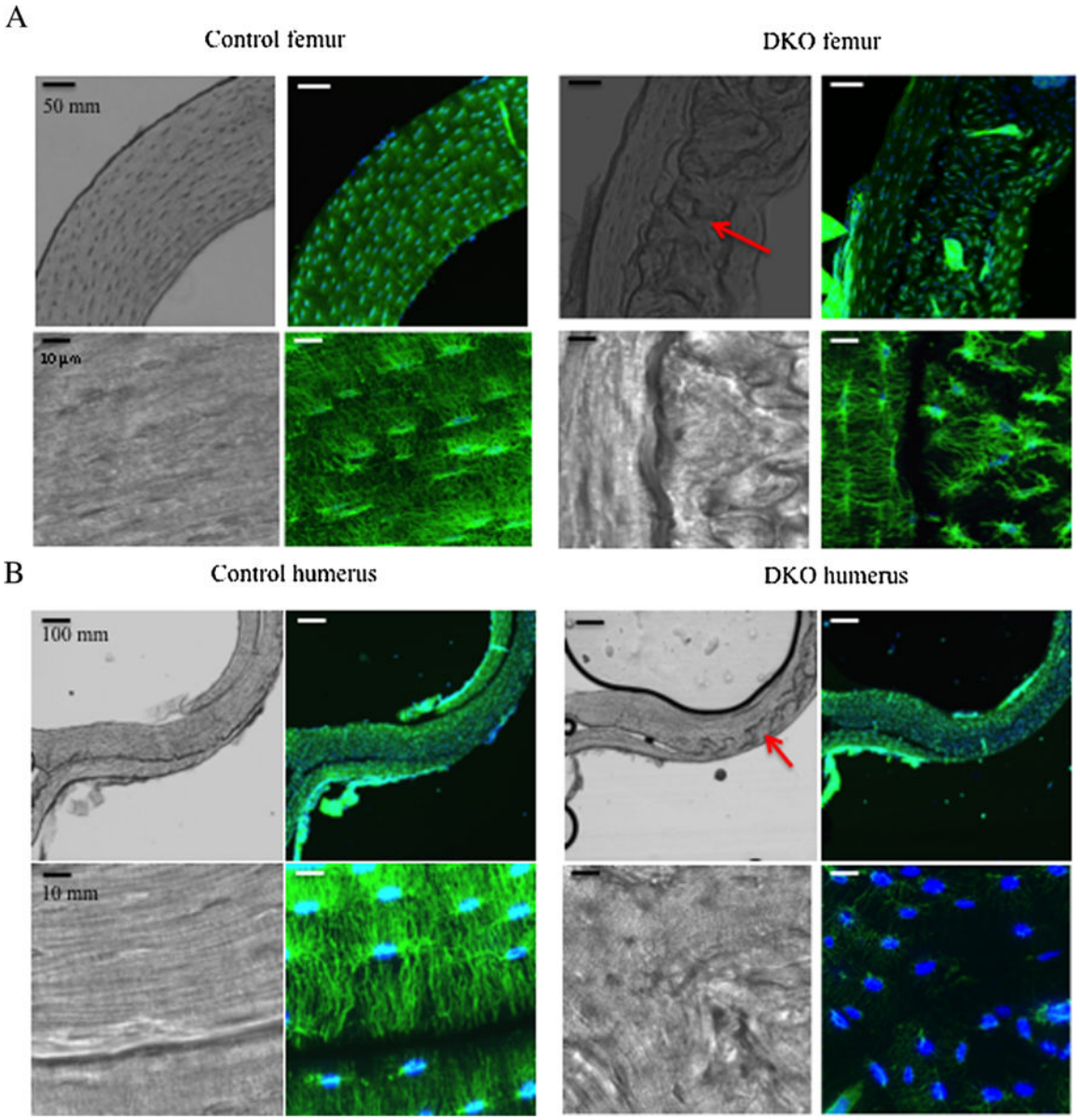


**Fig. 4.**

Disruption of the osteocytic network in DKO mice. (*A*) Upper panels: 10× magnification of femoral cortex in CTRL (left) and DKO (right) mice. The DAPI/phalloidin staining shows the abnormal osteocytic network in the DKO bone. Lower panels: 100× magnification of osteocytes in CTRL (left) and DKO (right) femoral cortex demonstrates discontinuities in the osteocyte network across the seams in the DKO bone found in the bright-field images in both the upper (red arrow) and lower panels. (B) Upper panels: 10× magnification of humeral cortex in CTRL (left) and DKO (right) mice. Lower panels: 100× magnification of osteocytes in CTRL (left) and DKO (right) humeral cortex demonstrates discontinuities in the osteocyte network across the seams on the DKO bone observed in the bright-field images

in both the upper third panel (red arrow) and lower third panels. The animals were 17 weeks old.

**Table 1**

Histomorphometric Analyses of Femoral Trabecular Bone in 4-Week-Old CTRL and DKO mice[a]

| Genotype | BV/TV (%) | TbTh (mcm) | TbSp (mcm) | OS/BS (%) | ObS/BS (%) | NOb/BPm (/mm) | NOb/Opm (/mm) | NOc/BPm (/mm) | OcS/BS (%) | NOc/TAR (#) |
|---|---|---|---|---|---|---|---|---|---|---|
| CTRL | 35.2 ± 3 | 22.9 ± 1 | 45.3 ± 5 | 29.6 ± 3 | 20.3 ± 2 | 20.9 ± 2 | 69.4 ± 2 | 2.5 ± 0 | 8.2 ± 1 | 62.2 ± 8 |
| DKO | 39.6 ± 3 | 20.2 ± 1 | 32.7 ± 4 | 20.0 ± 3 | 11.1 ± 2 | 11.5 ± 2 | 53.3 ± 7 | 1.6 ± 0 | 5.4 ± 1 | 50.2 ± 7 |
| % Change | +13 | −12 | −28 | −32 | −45 | −45 | −23 | −34 | −35 | −19 |
| *p* Value | 0.30 | 0.11 | 0.06 | 0.03 | 0.01 | 0.01 | 0.03 | 0.01 | 0.02 | 0.28 |

Values are mean ± SEM. $n = 10$ for CTRL and 9 for DKO.

[a]Measurements were obtained in the distal femur in an area of cancellous bone that measured ~2.5 $mm^2$, containing only secondary spongiosa and located 0.5 and 2.5 mm proximal to the epiphyseal growth cartilage.

**Table 2**

Cellular Response to PTH Treatment in DKO Mice[a]

| Genotype | OS/BS (%) | Obs/BS (%) | NOb/BPm (/mm) | NOc/BPm (/mm) | OcS/BS (%) | NOc/TAR (#) |
|---|---|---|---|---|---|---|
| WT VEH | 35.68 ± 7.0 | 17.55 ± 4.7 | 15.60 ± 4.3 | 1.27 ± 0.2 | 4.20 ± 0.5 | 10.63 ± 1.7 |
| WT PTH | 41.73 ± 2.9 | 22.51 ± 1.7 | 21.45 ± 2.0 | 1.66 ± 0.3 | 5.83 ± 1.0 | 23.97 ± 5.0 |
| *p* Value | 0.45 | 0.35 | 0.25 | 0.27 | 0.16 | 0.03 |
| DKO VEH | 5.142 ± 2.8 | 2.73 ± 1.7 | 2.754 ± 1.7 | 3.81 ± 1.1 | 13.38 ± 3.5 | 63.46 ± 11.9 |
| DKO PTH | 8.826 ± 3.0 | 5.17±1.9 | 5.142 ± 2.0 | 2.91 ± 0.3 | 10.35 ± 0.8 | 53.71 ± 6.4 |
| *p* Value | 0.40 | 0.36 | 0.38 | 0.44 | 0.42 | 0.49 |

Values are mean ± SEM. $n = 6$ for WT-VEH and 6 for WT-PTH. $n = 5$ for DKO-VEH and 5 for DKO-PTH.

[a]Measurements were obtained in the distal femur in an area of cancellous bone that measured ~2.5 $mm^2$, containing only secondary spongiosa and located 0.5 and 2.5 mm proximal to the epiphyseal growth cartilage.